RSC Advances

PAPER

View Article Online
View Journal | View Issue

Cite this: *RSC Adv.*, 2019, **9**, 24338

Thiophene-containing tetraphenylethene derivatives with different aggregation-induced emission (AIE) and mechanofluorochromic characteristics†

Ya Yin, Zhao Chen, * Yue Yang, Gang Liu, Congbin Fan and Shouzhi Pu*

Received 19th June 2019
Accepted 31st July 2019

DOI: 10.1039/c9ra04611a

rsc.li/rsc-advances

Four thiophene-containing tetraphenylethene derivatives were successfully synthesized and characterized. All these highly fluorescent compounds showed typical aggregation-induced emission (AIE) characteristics and emitted different fluorescence colors including blue-green, green, yellow and orange in the aggregation state. In addition, these luminogens also exhibited various mechanofluorochromic phenomena.

High-efficiency organic fluorescent materials have attracted widespread attention due to their potential applications in organic light-emitting devices and fluorescent switches.[1–8] Meanwhile, smart materials sensitive to environmental stimuli have also aroused substantial interest. Mechanochromic luminescent materials exhibiting color changes under the action of mechanical force (such as rubbing or grinding) are one important type of stimuli-responsive smart materials, which can be used as pressure sensors and rewritable media.[9–18] Bright solid-state emission and high contrast before and after grinding are very significant for the high efficient application of mechanochromic fluorescence materials.[19–28] However, a majority of traditional emissive materials usually exhibit poor emission efficiency in the solid state due to the notorious phenomenon of aggregation caused quenching (ACQ), and the best way to solve the problem is to develop a class of novel luminescent materials oppositing to the luminophoric materials with ACQ effect. Fortunately, an unusual aggregation-induced emission (AIE) phenomenon was discovered by Tang *et al.* in 2001.[29] Indeed, the light emission of an AIE-active compound can be enhanced by aggregate formation.[30–32] Obviously, it is possible that AIE-active mechanochromic fluorescent compounds can be applied to the preparation of high-efficiency mechanofluorochromic materials. Numerous luminescent materials exhibiting mechanochromic fluorescent behavior have been discovered up to now.[33] Whereas, examples of fluorescent molecules simultaneously possessing AIE and mechanofluorochromic behaviors are still limited, and the exploitation of more AIE-active mechanofluorochromic luminogens is necessary. Organic solid emitters with twisted molecular conformation can effectively prevent the formation of ACQ effect, thus exhibiting strong solid-state luminescence. Tetraphenylethene is a highly twisted fluorophore. Meanwhile, it is also a typical AIE unit, which can be used to construct high emissive stimuli-responsive functional materials.[34–37]

The design and synthesis of novel organic emitters with tunable emission color has become a promising research topic at present. Only a limited number of organic fluorescent materials with full-color emission have been reported to date.[38,39] For example, in 2018, Tang *et al.* reported six tetraphenylpyrazine-based compounds. Interestingly, in film states, these luminogens exhibited different fluorescence colors covering the entire visible range, and this is the first example of realizing full-color emission based on the tetraphenylpyrazine unit.[40] It is still an urgent challenge to develop novel organic luminophors with tunable emission color basing on the same core structure.

In this study, four organic fluorophores containing tetraphenylethene unit were successfully synthesized (Scheme 1). Introducing the thiophene and carbonyl units into the molecules possibly promoted the formation of weak intermolecular interactions such as C–H···S or C–H···O interaction, which was advantageous to the exploitation of interesting stimuli-responsive fluorescent materials. Indeed, all these compounds showed obvious AIE characteristics. Furthermore, these luminogens emitted a series of different fluorescent colors involving blue-green, green, yellow and orange in the aggregation state. In addition, these luminogens also exhibited reversible mechanofluorochromic phenomena involving different fluorescent color changes.

To investigate the aggregation-induced properties of compounds **1–4**, the UV-vis absorption spectra of **1**, **2**, **3** and **4**

Jiangxi Key Laboratory of Organic Chemistry, Jiangxi Science and Technology Normal University, Nanchang 330013, PR China. E-mail: chenzhao666@126.com; pushouzhi@tsinghua.org.cn

† Electronic supplementary information (ESI) available: Experimental section, NMR spectra, mass spectra, and characterization data mentioned in the paper. CCDC 1935026 and 1935027. For ESI and crystallographic data in CIF or other electronic format see DOI: 10.1039/c9ra04611a

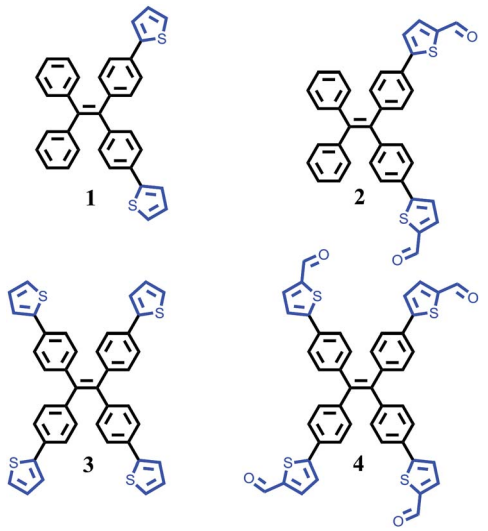

Scheme 1 The molecular structures of compounds **1–4**.

(20 μM) in DMF–H_2O mixtures of varying proportions were studied initially (Fig. S1†). Obviously, level-off tails were obviously observed in the long-wavelength region as the water content increased. This interesting phenomenon is generally associated with the formation of nano-aggregates.[41] Next, the photoluminescence (PL) spectra of **1–4** in DMF–H_2O mixtures with various water fraction (f_w) values were explored. As shown in Fig. 1, almost no PL signals were noticed when a diluted DMF solution of luminogen **1** was excited at 365 nm, and thus almost no fluorescence could be observed upon UV illumination at 365 nm, and the corresponding absolute fluorescence quantum yield (Φ) was as low as 0.04%. However, when the water content was increased to 50%, a new blue-green emission band with a λ_{max} at 501 nm was observed, and a faint blue-green fluorescence was noticed under 365 nm UV light. As the water content was further increased to 90%, a strong blue-green emission (Φ = 30.81%) could be observed. Furthermore, as shown in Fig. S2,† the nano-aggregates (f_w = 90%) obtained were confirmed by dynamic light scattering (DLS). Therefore, the compound **1** with bright blue-green emission caused by aggregate formation showed typical AIE feature.

Similarly, as can be seen in Fig. 2–4, compounds **2–4** also showed obvious aggregation-induced green emission, aggregation-induced yellow emission, and aggregation-induced orange emission, respectively. When the water content was zero, the quantum yields of compounds **2–4** were 0.04%, 0.05% and 0.46%, respectively, while as the water content increased to 90%, the corresponding quantum yields of compounds **2–4** also increased to 30.67%, 45.57% and 26.53%, respectively. Hence, luminogens **2–4** were also AIE-active species. In addition, as shown in Fig. 5, the DFT calculations for the compounds **1–4** were performed. The calculated energy gaps (ΔE) of four compounds were 3.6178416 eV (compound **1**), 3.276084 eV (compound **2**), 3.3073755 eV (compound **3**) and 3.0766347 eV (compound **4**) respectively. Therefore, the various numbers and the various kinds of the substituents had slight effects on their molecular orbital energy levels of **1–4**.

Subsequently, the mechanochromic fluorescent behaviors of compounds **1–4** were surveyed by solid-state PL spectroscopy. As shown in Fig. 6, the as-synthesized powder sample **1** exhibited an emission band with a λ_{max} at 444 nm, corresponding to a blue fluorescence under 365 nm UV light. Intriguingly, a new blue-green light-emitting band with a λ_{max} at 507 nm was observed after the pristine solid sample was ground. After fuming with dichloromethane solvent vapor for 1 min, the blue-green fluorescence was converted back to the

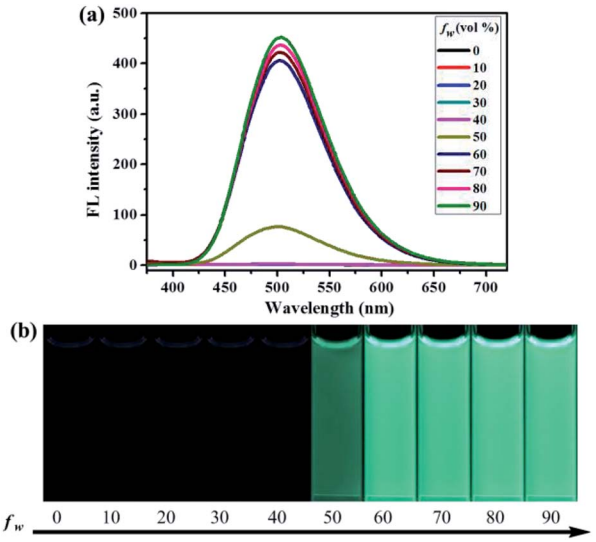

Fig. 1 (a) Fluorescence spectra of the dilute solutions of compound **1** (2.0×10^{-5} mol L^{-1}) in DMF–water mixtures with different water contents (0–90%). Excitation wavelength = 365 nm. (b) Fluorescence images of **1** (2.0×10^{-5} mol L^{-1}) in DMF–water mixtures with different f_w values under 365 nm UV light.

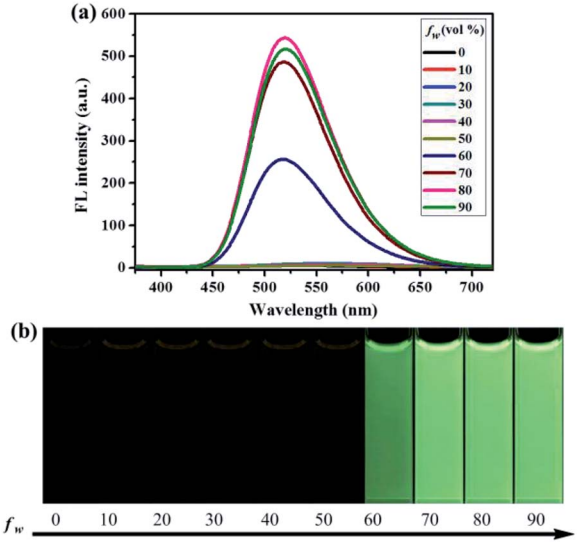

Fig. 2 (a) Fluorescence spectra of the dilute solutions of compound **2** (2.0×10^{-5} mol L^{-1}) in DMF–water mixtures with different water contents (0–90%). Excitation wavelength = 365 nm. (b) Fluorescence images of **2** (2.0×10^{-5} mol L^{-1}) in DMF–water mixtures with different f_w values under 365 nm UV light.

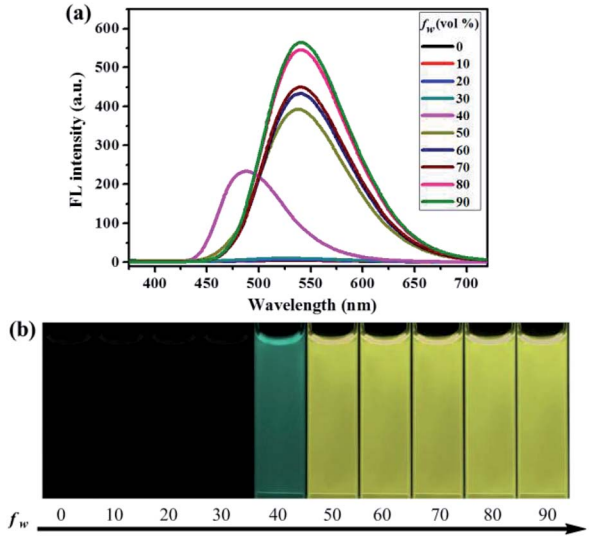

Fig. 3 (a) Fluorescence spectra of the dilute solutions of compound **3** (2.0×10^{-5} mol L^{-1}) in DMF–water mixtures with different water contents (0–90%). Excitation wavelength = 365 nm. (b) Fluorescence images of **3** (2.0×10^{-5} mol L^{-1}) in DMF–water mixtures with different f_w values under 365 nm UV light.

original blue fluorescence. Therefore, luminogen **1** exhibited reversible mechanochromic fluorescence feature. Furthermore, this reversible mechanofluorochromic conversion was repeated many times by grinding-exposure without showing signs of fatigue (Fig. 10).

Similarly, as evident from Fig. 7–9, luminogens **2–4** also exhibited obvious mechanofluorochromic characteristics. Moreover, the repeatabilities of their mechanochromic behaviors were also satisfactory (Fig. S3†). Hence, all the compounds **1–4** showed reversible mechanofluorochromic phenomena

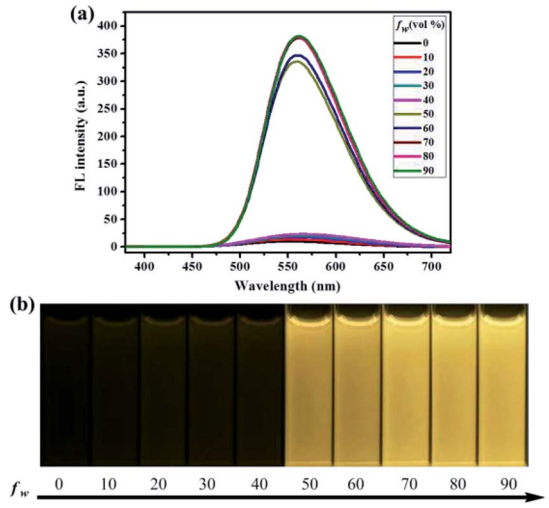

Fig. 4 (a) Fluorescence spectra of the dilute solutions of compound **4** (2.0×10^{-5} mol L^{-1}) in DMF–water mixtures with different water contents (0–90%). Excitation wavelength = 365 nm. (b) Fluorescence images of **4** (2.0×10^{-5} mol L^{-1}) in DMF–water mixtures with different f_w values under 365 nm UV light.

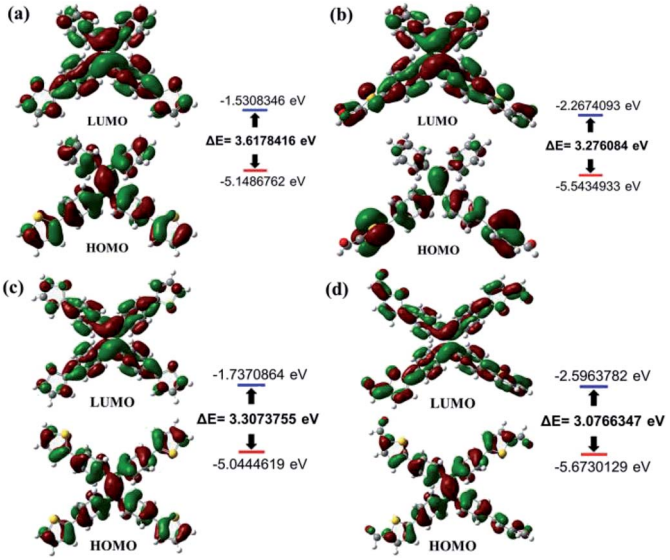

Fig. 5 (a) HOMO and LUMO frontier molecular orbitals of molecule **1** based on DFT (B3LYP/6-31G*) calculation. (b) HOMO and LUMO frontier molecular orbitals of molecule **2** based on DFT (B3LYP/6-31G*) calculation. (c) HOMO and LUMO frontier molecular orbitals of molecule **3** based on DFT (B3LYP/6-31G*) calculation. (d) HOMO and LUMO frontier molecular orbitals of molecule **4** based on DFT (B3LYP/6-31G*) calculation.

involving different fluorescent color changes, and the various numbers of the substituents could effectively influence the mechanofluorochromic behaviors of **1–4**. Obviously, luminogen **3** or **4** after grinding exhibited more red-shifted fluorescence in comparison with that of the corresponding luminogen **1** or **2** after grinding.

In order to further explore the possible mechanism of mechanofluorochromism of **1–4**, the powder X-ray diffraction (PXRD) measurements of various solid states of **1–4** were carried out. As depicted in Fig. 11, the pristine solid powder **1** showed many clear and intense reflection peaks, suggesting its crystalline phase. However, after the pristine powder sample was ground, the sharp and intense diffraction peaks vanished,

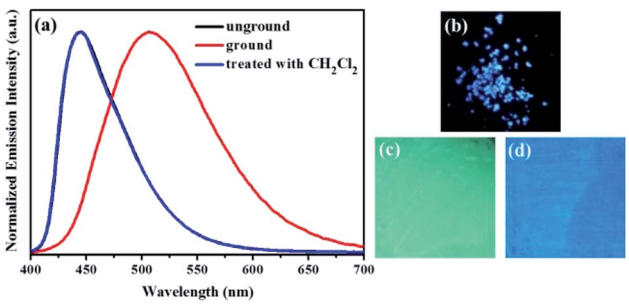

Fig. 6 (a) Solid-state PL spectra of compound **1** before grinding, after grinding, and after treatment with dichloromethane solvent vapor. Excitation wavelength: 365 nm. Photographic images of compound **1** under 365 nm UV light: (b) the as-synthesized powder sample. (c) The ground sample. (d) The sample after treatment with dichloromethane solvent vapor.

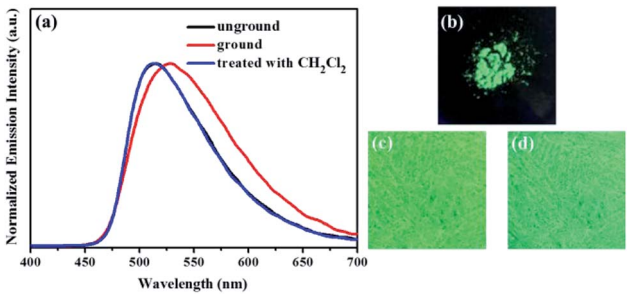

Fig. 7 (a) Solid-state PL spectra of compound **2** before grinding, after grinding, and after treatment with dichloromethane solvent vapor. Excitation wavelength: 365 nm. Photographic images of compound **2** under 365 nm UV light: (b) the as-synthesized powder sample. (c) The ground sample. (d) The sample after treatment with dichloromethane solvent vapor.

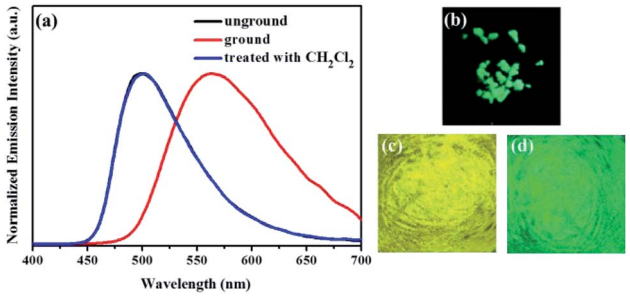

Fig. 8 (a) Solid-state PL spectra of compound **3** before grinding, after grinding, and after treatment with dichloromethane solvent vapor. Excitation wavelength: 365 nm. Photographic images of compound **3** under 365 nm UV light: (b) the as-synthesized powder sample. (c) The ground sample. (d) The sample after treatment with dichloromethane solvent vapor.

which indicated the crystalline form was converted to the amorphous form. Interestingly, when the ground solid sample was fumigated with dichloromethane solvent vapor for 1 min, the corresponding sample powder exhibited the PXRD pattern of the initial crystalline form. Meanwhile, the structural transformations of the solid samples of **2–4** were similar to that of **1**

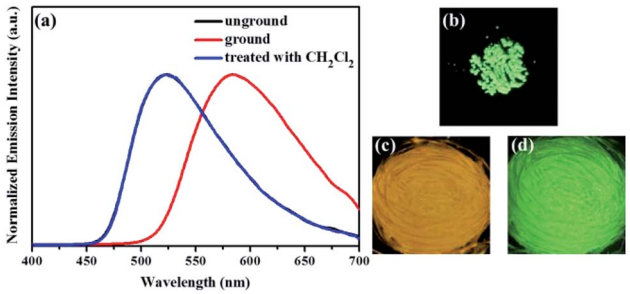

Fig. 9 (a) Solid-state PL spectra of compound **4** before grinding, after grinding, and after treatment with dichloromethane solvent vapor. Excitation wavelength: 365 nm. Photographic images of compound **4** under 365 nm UV light: (b) the as-synthesized powder sample. (c) The ground sample. (d) The sample after treatment with dichloromethane solvent vapor.

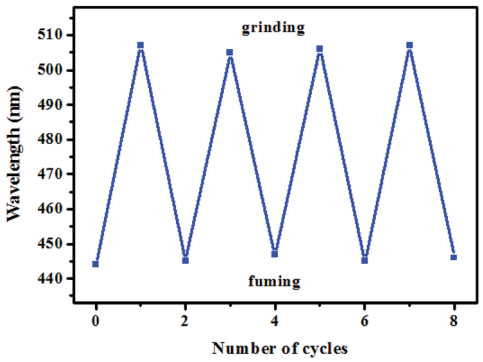

Fig. 10 Repetitive experiment of mechanochromic behavior for compound **1**.

(Fig. S4–S6†). Obviously, the morphological changes of solid samples of **1–4** from crystalline state to amorphous state and *vice versa* could be attributed to the reversible mechanical switching in compounds **1–4**, and the mechanofluorochromic phenomena observed in **1–4** were related to the morphological transition involving the ordered crystalline phase and the disordered amorphous phase.

Fortunately, single crystals of compounds **1** and **2** were obtained by slow diffusion of *n*-hexane into a trichloromethane solution containing small amounts of **1** or **2**. As shown in Fig. 12 and 13, the molecular structures of **1** and **2** exhibited a twisted conformation due to the existence of tetraphenylethene unit. Meanwhile, some weak intermolecular interactions, such as C–H···π interaction (d = 2.866 Å) for **1**, π···π interaction (d = 3.371 Å) for **1**, C–H···S interaction (d = 2.977 Å) for **2**, and π···π interaction (d = 3.189 Å) for **2**, were observed. These weak intermolecular interactions gave rise to a loose packing motif of **1** or **2**, which indicated their ordered crystal packings might readily collapse upon exposure to external mechanical stimulus. Therefore, their solid-state fluorescence could be adjusted by mechanical force.

In summary, four fluorescent molecules containing thiophene and tetraphenylethene units were successfully designed and synthesized in this study. All these compounds showed obvious AIE characteristics. Furthermore, these luminogens

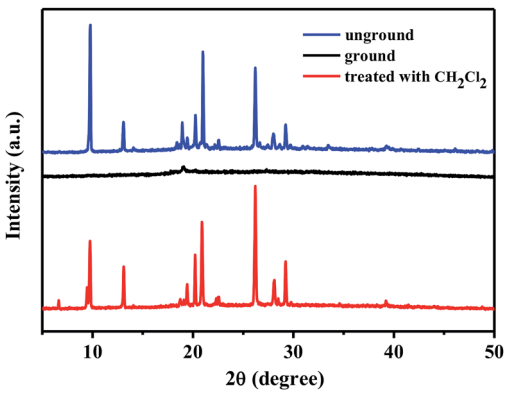

Fig. 11 XRD patterns of compound **1**: unground, ground and after treatment with dichloromethane solvent vapor.

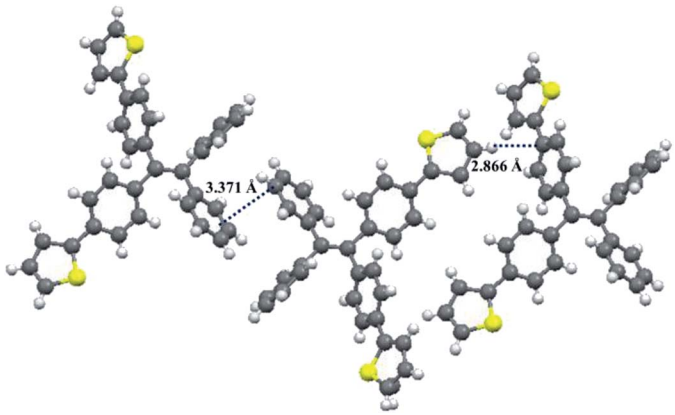

Fig. 12 The structural organization of compound **1**.

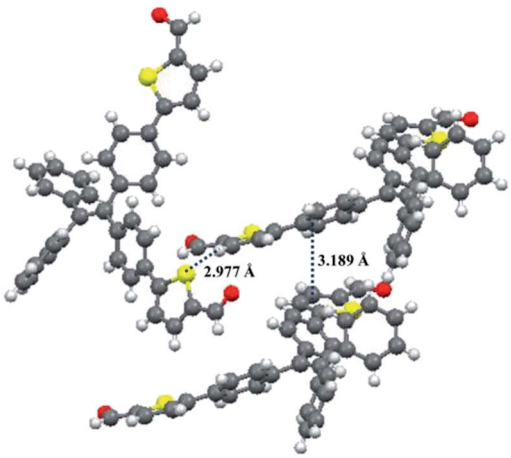

Fig. 13 The structural organization of compound **2**.

emitted various fluorescence colors involving blue-green, green, yellow and orange in the aggregation state. Meanwhile, these luminogens basing on the same core structure also exhibited reversible mechanofluorochromic phenomena involving different fluorescent color changes. The results of this study will be beneficial for the exploitation of novel luminophors with full-color emission.

Conflicts of interest

There are no conflicts to declare.

Acknowledgements

The authors are grateful for the financial support from the National Natural Science Foundation of China (21702079 and 41867053), the "5511" Science and Technology Innovation Talent Project of Jiangxi Province (20165BCB18015), the Key Project of Natural Science Foundation of Jiangxi Province (20171ACB20025), the Youth Project of Natural Science Foundation of Jiangxi Province (20171BAB213004), the Young Talents Project of Jiangxi Science and Technology Normal University (2017QNBJRC005), and the Project of the Science Fund of Jiangxi Education Office (GJJ180593).

Notes and references

1 Y. Hong, J. W. Y. Lam and B. Z. Tang, *Chem. Soc. Rev.*, 2011, **40**, 5361–5388.
2 Z. Chen, J. Liang, X. Han, J. Yin, G. A. Yu and S. H. Liu, *Dyes Pigm.*, 2015, **112**, 59–66.
3 L. Wang, T. Yu, Z. Xie, E. Ubba, T. Zhan, Z. Yang, Y. Zhang and Z. Chi, *RSC Adv.*, 2018, **8**, 18613–18618.
4 S. Lee, H. Shin and J. J. Kim, *Adv. Mater.*, 2014, **26**, 5864–5868.
5 Y. Liu, M. Nishiura, Y. Wang and Z. Hou, *J. Am. Chem. Soc.*, 2006, **128**, 5592–5593.
6 Z. Chen, D. Wu, X. Han, J. Liang, J. Yin, G. A. Yu and S. H. Liu, *Chem. Commun.*, 2014, **50**, 11033–11035.
7 Y. Sun, F. Ding, Z. X. Zhou, C. L. Li, M. P. Pu, Y. L. Xu, Y. Zhan, X. J. Lu, H. B. Li, G. F. Yang, Y. Sun and P. J. Stang, *Proc. Natl. Acad. Sci. U. S. A.*, 2019, **116**, 1968–1973.
8 J. H. Chen, F. Y. Ye, Y. Lin, Z. Chen, S. H. Liu and J. Yin, *Sci. China: Chem.*, 2019, **62**, 440–450.
9 Z. Chen, J. Zhang, M. Song, J. Yin, G. A. Yu and S. H. Liu, *Chem. Commun.*, 2015, **51**, 326–329.
10 Z. Chen, G. Liu, S. Pu and S. H. Liu, *Dyes Pigm.*, 2017, **143**, 409–415.
11 M. Fang, J. Yang, Q. Liao, Y. Gong, Z. Xie, Z. Chi, Q. Peng, Q. Li and Z. Li, *J. Mater. Chem. C*, 2017, **5**, 9879–9885.
12 J. Chen, D. Li, W. Chi, G. Liu, S. H. Liu, X. Liu, C. Zhang and J. Yin, *Chem.–Eur. J.*, 2018, **24**, 3671–3676.
13 Y. Yin, F. Zhao, Z. Chen, G. Liu and S. Pu, *Tetrahedron Lett.*, 2018, **59**, 4416–4419.
14 B. Xu, Y. Mu, A. Mao, Z. Xie, H. Wu, Y. Zhang, C. Jin, Z. Chi, S. Liu, J. Xu, Y. C. Wu, P. Y. Lu, A. Lien and M. R. Bryce, *Chem. Sci.*, 2016, **7**, 2201–2206.
15 W. Chen, S. Wang, G. Yang, S. Chen, K. Ye, Z. Hu, Z. Zhang and Y. Wang, *J. Phys. Chem. C*, 2016, **120**, 587–597.
16 Y. Dong, B. Xu, J. Zhang, X. Tan, L. Wang, J. Chen, H. Lv, S. Wen, B. Li, L. Ye, B. Zhou and W. Tian, *Angew. Chem., Int. Ed.*, 2012, **51**, 10782–10785.
17 P. Xue, J. Ding, P. Wang and R. Lu, *J. Mater. Chem. C*, 2016, **4**, 6688–6706.
18 A. Tang, Z. Chen, G. Liu and S. Pu, *Tetrahedron Lett.*, 2018, **59**, 3600–3604.
19 Z. Chen, J. Liang, Y. Nie, X. Xu, G. A. Yu, J. Yin and S. H. Liu, *Dalton Trans.*, 2015, **44**, 17473–17477.
20 Z. Chen, Y. Nie and S. H. Liu, *RSC Adv.*, 2016, **6**, 73933–73938.
21 Z. Chen, G. Liu, S. Pu and S. H. Liu, *Dyes Pigm.*, 2018, **159**, 499–505.
22 F. Zhao, Z. Chen, G. Liu, C. Fan and S. Pu, *Tetrahedron Lett.*, 2018, **59**, 836–840.
23 Y. Qi, Y. Wang, Y. Yu, Z. Liu, Y. Zhang, G. Du and Y. Qi, *RSC Adv.*, 2016, **6**, 33755–33762.
24 X. Han, Y. Liu, G. Liu, J. Luo, S. H. Liu, W. Zhao and J. Yin, *Chem.–Asian J.*, 2019, **14**, 890–895.

25 T. Lin, X. Su, K. Wang, M. Li, H. Guo, L. Liu, B. Zhou, Y. M. Zhang, Y. Liu and S. X. A. Zhang, *Mater. Chem. Front.*, 2019, **3**, 1052–1061.
26 H. Ito, T. Saito, N. Oshima, N. Kitamura, S. Ishizaka, Y. Hinatsu, M. Wakeshima, M. Kato, K. Tsuge and M. Sawamura, *J. Am. Chem. Soc.*, 2008, **130**, 10044–10045.
27 R. Yadav, A. Rai, A. K. Sonkar, V. Rai, S. C. Gupta and L. Mishra, *New J. Chem.*, 2019, **43**, 7109–7119.
28 S. Sinha, B. Chowdhury, U. K. Ghorai and P. Ghosh, *Chem. Commun.*, 2019, **55**, 5127–5130.
29 J. D. Luo, Z. L. Xie, J. W. Y. Lam, L. Cheng, H. Y. Chen, C. F. Qiu, H. S. Kwok, X. W. Zhan, Y. Q. Liu, D. B. Zhu and B. Z. Tang, *Chem. Commun.*, 2001, 1740–1741.
30 J. Mei, Y. Hong, J. W. Y. Lam, A. Qin, Y. Tang and B. Z. Tang, *Adv. Mater.*, 2014, **26**, 5429–5479.
31 J. Mei, N. L. C. Leung, R. T. K. Kwok, J. W. Y. Lam and B. Z. Tang, *Chem. Rev.*, 2015, **115**, 11718–11940.
32 J. Liang, B. Z. Tang and B. Liu, *Chem. Soc. Rev.*, 2015, **44**, 2798–2811.
33 R. Tan, S. Wang, H. Lan and S. Xiao, *Curr. Org. Chem.*, 2017, **21**, 236–248.
34 S. M. Wagalgave, S. V. Bhosale, R. S. Bhosale, A. L. Puyad, J. Y. Chen, J. L. Li, R. A. Evans, A. Gupta and S. V. Bhosale, *Mater. Chem. Front.*, 2019, **3**, 1231–1237.
35 F. Zhao, C. Fan, Z. Chen, G. Liu and S. Pu, *RSC Adv.*, 2017, **7**, 43845–43848.
36 B. Yuan, D. X. Wang, L. N. Zhu, Y. L. Lan, M. Cheng, L. M. Zhang, J. Q. Chu, X. Z. Li and D. M. Kong, *Chem. Sci.*, 2019, **10**, 4220–4226.
37 F. K. Zhan, J. C. Liu, B. Cheng, Y. C. Liu, T. S. Lai, H. C. Lin and M. Y. Yeh, *Chem. Commun.*, 2019, **55**, 1060–1063.
38 Y. Kubota, Y. Ozaki, K. Funabiki and M. Matsui, *J. Org. Chem.*, 2013, **78**, 7058–7067.
39 S. Y. Lee, T. Yasuda, Y. S. Yang, Q. Zhang and C. Adachi, *Angew. Chem., Int. Ed.*, 2014, **53**, 6402–6406.
40 L. Pan, Y. Cai, H. Wu, F. Zhou, A. Qin, Z. Wang and B. Z. Tang, *Mater. Chem. Front.*, 2018, **2**, 1310–1316.
41 C. W. T. Leung, Y. Hong, S. Chen, E. Zhao, J. W. Y. Lam and B. Z. Tang, *J. Am. Chem. Soc.*, 2013, **135**, 62–65.